Inwave: a new flexible design tool dedicated to wave energy converters

Adrien Combourieu, Maxime Philippe, François Rongère, Aurélien Babarit

INWAVE: A NEW FLEXIBLE DESIGN TOOL DEDICATED TO WAVE ENERGY CONVERTERS

Adrien Combourieu
INNOSEA
Nantes, France

Maxime Philippe
INNOSEA
Nantes, France

François Rongère
LUNAM Université
Ecole Centrale de Nantes - CNRS
Nantes, France

Aurélien Babarit
LUNAM Université
Ecole Centrale de Nantes - CNRS
Nantes, France

ABSTRACT

This article presents the novel methodology used in the software *InWave* to address the problem of wave energy converters (WEC) modelling. The originality compared to other recently developed tools lies in a fast semi-recursive multi-body dynamic solver which integrates a flexible hydrodynamic solver.

The multibody solver works in time domain and is fully nonlinear. It solves the dynamic of systems formed of a fixed or free base articulated with any number of bodies that can be floating or not, with branchy structure ([1]).

The integrated hydrodynamic solver is a linear potential flow solver based on boundary elements method. It uses the generalized degrees of freedom approach ([11]). Combined with a relative coordinate parameterization, it allows for a minimization of the number of hydrodynamic boundary value problems that have to be solved, thus allowing a reduction of computational time both for BEM computations and time domain simulations. Time domain reconstruction is performed to link hydrodynamic loads with the multibody dynamic solver. Interaction between bodies through radiation is thus taken into account.

InWave is a complete WEC modelling tool including incident wave generation, multibody dynamic solver, hydrodynamic solver, power take-off and mooring models, post-processing and visualization.

A successful comparison with the linear potential flow solver *Aquaplus* ([5]) on a basic cylinder test case is carried out.

Finally, a complex test case on a Langlee-like device is presented, comparing *InWave* results with those from the *NumWec* project ([2]). A good agreement between both models is found, which increases the confidence in *InWave* algorithms and implementation.

NOMENCLATURE

n_{bodies}	number of bodies
n_{joints}	number of articulations
$n_{dof} = 6 + n_{joints}$	number of DoFs
$\boldsymbol{\eta}$	(6×1)base body position
$\boldsymbol{q}$	$(n_{joints} \times 1)$articulations position
$\boldsymbol{Y}$	$(n_{dof} \times 1)$ multibody position
$\boldsymbol{H}$	$(n_{dof} \times n_{dof})$ multibody inertia matrix
$\boldsymbol{H_a^\infty}$	$(n_{dof} \times n_{dof})$ multibody added mass matrix
$\boldsymbol{\mu}$	$(n_{dof} \times 1)$ radiation damping load on multibody
$\boldsymbol{C}$	$(n_{dof} \times 1)$ external loads on multibody
$\boldsymbol{\Gamma}$	$(n_{joints} \times 1)$ PTO loads in articulations
$\boldsymbol{B}$	$(n_{dof} \times n_{dof})$ multibody radiation damping matrix
$\boldsymbol{K_{rad}}$	$(n_{dof} \times n_{dof})$ radiation impulse response matrix
$\boldsymbol{K_{diff}}$	(6×1) diffraction impulse response on each body

INTRODUCTION

More and more often, new wave energy converters (WEC) are proposed which involve a large number of bodies linked in various ways. These systems are difficult to model numerically

with conventional seakeeping softwares for different reasons. First, the links between bodies makes the motion equations specific to each system. In addition, unusual degrees of freedom (DoFs) are at stake, which are not easy to input directly.

This issue started being addressed in the last few years, mainly by *DNV-GL* with *WaveDyn* software ([4]). Other work on the subject was carried out by *NREL* and *Sandia National Laboratories* ([7]) and *Re Vision Consulting, LLC* ([8]). Because of the large number of environmental conditions to be tested in WEC designs, linear potential flow solvers using Boundary Elements Method (BEM) are unanimously used for their low computational time.

Up to now, the method consisted in treating each body independently in 6 DoFs in the BEM. The links between bodies are later expressed as constraints in the time domain dynamic equation. This approach is not optimal both for the BEM solver and the time domain simulation.

The novelty of *InWave* lies in a multibody dynamic solver which is able to build and solve directly the dynamic equation for a multibody tree structure. Moreover, contrary to [4], [8] that call conventional commercial BEM softwares (*WAMIT*), *InWave* integrates a flexible hydrodynamic solver.

In the following, the novel numerical model implemented by *InWave* is first exposed. Verification is carried out on a simple cylinder test case, comparing *InWave* with conventional seakeeping code *Aquaplus* ([5]). Finally, a complex test case on a *Langlee*-like device is presented, comparing *InWave* results with those from the *NumWec* project ([2]).

NUMERICAL MODEL

In this section, the different modules of *InWave* are described, and in particular the links between each other's.

Overview

InWave is a complete tool dedicated to WECs modeling. It is composed of few fully integrated main modules:

- **Multibody structure description:** It allows describing the WEC structure as a number of bodies linked with each other's by various links. The multibody structure is represented with a minimal set of degrees of freedom thanks to an efficient representation based on modified Denavit-Hartenberg parameterization [6].
- **Multibody dynamic solver:** it solves the motion of arbitrary branched-articulated multibody structures in time domain. It relies on fast nonlinear semi-recursive algorithms derived from robotics. It supports any kind of input forces on bodies or articulations (Power Take-Off). Depending on the forces activated, this module is able:
    - To find the hydrostatic equilibrium position of the multibody structure by dynamic relaxation. This hydrostatic equilibrium position is needed by the hydrodynamic solver. It also computes the hydrostatic data of the structure at equilibrium.
    - To perform simulations in waves.
    - To perform decay tests.
- **Hydrodynamic solver:** This module solves the hydrodynamic loads on each body of the multibody structure. It is a linear potential flow solver based on BEM, fully integrated in *InWave* code. It uses the generalized degrees of freedom approach. Combined with a minimal number of DOFs, it allows for a minimization of the number of hydrodynamic boundary value problems that have to be solved. It provides hydrodynamic data needed by the multibody solver to compute radiation and wave excitation loads.
- **Ocean:** This module is responsible of incident wave generation as input for the multibody solver. It implements different wave models.
- **PTO and moorings:** allows user to define the Power Take-Offs and mooring system. This information is used as input of the multibody solver.
- **Post-Processing environment**: it processes time series generated by the multibody solver to get high level results (RAOs, extracted power…).

The organization of the different modules is depicted in Figure 1.

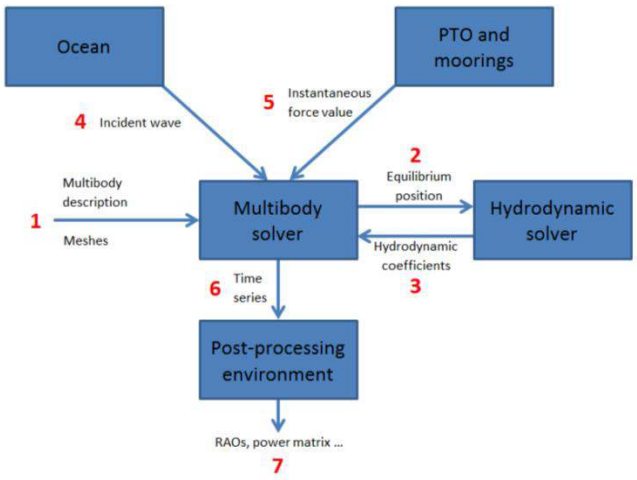

Figure 1: Software organization

From the user point of view, the sequential process is as follows:

1. User inputs the multibody structure description and the bodies' meshes.
2. The equilibrium position of the system is found by the multibody dynamic solver and is sent to the hydrodynamic solver.
3. Hydrodynamic solver computes radiation/diffraction coefficients in frequency domain. Those coefficients are processed to get time domain impulse responses.
4. Wave model is chosen.

5. PTO and moorings models are input.
6. The multibody solver computes the motion of the WEC system in waves, with active mooring and PTOs.
7. Time series are post processed to obtain high level results and visualizations.

The multibody structure description

The multibody WEC system is concisely defined using an efficient description issued from robotics: the modified Denavit-Hartenberg parameters ([1], [6]). This set of parameters (a 6D vector for each body) describes the bodies' relative positions and how they are linked to each other's. The multibody structure is modelled as a base body moving in 6 DoFs along with a chain of n_{joints} articulated bodies. In total, the structure has $n_{dof} = 6 + n_{joints}$ DoFs (see Figure 2). Its position can thus be represented by a $(n_{dof} \times 1)$ vector:

$$\boldsymbol{Y} = \begin{bmatrix} \boldsymbol{\eta} \\ \boldsymbol{q} \end{bmatrix} \quad (1)$$

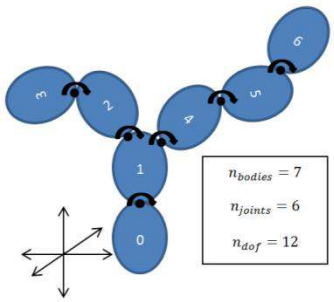

Figure 2: Visualization of multibody DoFs

The multibody dynamic solver

The multibody solver module works in time domain and is fully nonlinear. It solves the direct dynamic problem for a multibody structure. It means that given the forces acting on the structure, it obtains its kinematics. At that level, no particular assumption is made on loads model.

The implementation is made in C++ in an Object Oriented manner. Details of the algorithms are described in ([1]).

The inputs of this module are:

- The full description of the multibody structure (inertial data, modified Denavit-Hartenberg parameters).
- The definition of external forces acting on bodies.
- The definition of forces or torques acting on articulations.

Note that all internal inertial forces are automatically accounted for by the solver.

Then, at each time step, the solver builds and solves the multibody motion equation ([3]):

$$\begin{bmatrix} \mathbf{0}_{6\times1} \\ \boldsymbol{\Gamma} \end{bmatrix} = (\boldsymbol{H} + \boldsymbol{H}_{\boldsymbol{a}}^{\infty})\ddot{\boldsymbol{Y}} + \boldsymbol{C}(\boldsymbol{Y}, \dot{\boldsymbol{Y}}) + \boldsymbol{\mu}(\dot{\boldsymbol{Y}}) \quad (2)$$

It is important to note that equation (2) directly describes the multibody structure motion. Here lies one of the main assets of *InWave* compared to other approaches which solve the motion of each body with kinematic constraints.

In (2), matrix $\boldsymbol{H}$ $(n_{dof} \times n_{dof})$ and vector $\boldsymbol{C}$ (n_{dof}) are built using a recursive algorithm derived from robotics ([1]). The solver linearly walks through the tree structure to build these quantities. $\boldsymbol{H}$ is the inertia matrix of the multibody structure. It is not constant and varies with the position of the multibody system. $\boldsymbol{C}$ vector gathers the external forces acting on each body. It takes into account the propagation of loads in the multibody structure. Wave excitation and diffraction are included in this vector. Specific loads models can be introduced here (e.g. Morison drag for viscous damping model in the F3OF study).

$\boldsymbol{H}_{\boldsymbol{a}}^{\infty}$ $(n_{dof} \times n_{dof})$ and $\boldsymbol{\mu}$ (n_{dof}) account for radiation loads. $\boldsymbol{H}_{\boldsymbol{a}}^{\infty}$ represents the added mass of the multibody structure. As hydrodynamic coefficients are computed only at equilibrium, it is supposed to be constant. $\boldsymbol{\mu}$ is the hydrodynamic damping acting on each DoF. It is computed at each time step (see equation (6)).

Radiation loads had to be treated specifically for two reasons:

- The loads due to added mass are proportional to accelerations, which is the unknown of equation (2)
- The damping load acting on a given body is linked to the velocities of all other bodies. This coupling is more naturally expressed at the scale of the multibody structure rather than at body level.

Finally, the left-hand side of (2) represents the PTO forces acting on each articulation (thus usually $\mathbf{0}_{6\times1}$ for base DoFs).

Equation (2) is integrated using Adams-Moulton algorithm with an adaptive time step. Integration therefore slows down when dynamic is complex and accelerates when it is easy to solve, ensuring accuracy.

The equilibrium position research

For complex structures as WECs, the hydrostatic equilibrium position is *a priori* unknown. *InWave* finds it by running a dynamic relaxation in still water. Only gravity and nonlinear buoyancy are activated at this stage.

From a user input initial position, the system evolves to one equilibrium position. Numerical damping is used to dissipate the excess of potential energy of the initial position and enable convergence.

Once the equilibrium position is found, the linear hydrostatic is computed and the linear potential flow solver can be run (see Figure 1).

Hydrodynamic modelling

From the multibody structure at equilibrium, a mesh of the wetted surface is extracted for calculation of the hydrodynamic coefficients. The open source linear potential flow solver Nemoh [12], an evolution of the former seakeeping code

Aquaplus [5] is used. Basically, Nemoh solves the linear boundary value problem for a given distribution of the normal velocity on the panels of the mesh. Hence, the normal velocities are calculated in preprocessing by the multibody solver for the various diffraction and radiation problems which need to be considered.

Indeed, the multibody solver makes the structure move with a unit velocity along each of the DoF independently. When a body moves along its DoF, the following bodies move with it. For example, when the base is moving along one of its 6 DoF, the whole structure is moving with it (see Figure 3). Doing so, the velocity of each face center along the face normal are recorded by the multibody solver and given as boundary condition to Nemoh for radiation problems.

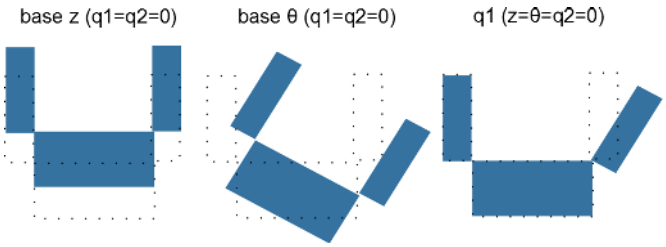

Figure 3: Example of a multibody structure motion for radiation problems definition

Concerning diffraction problems, the boundary conditions are simply deduced from fluid velocity on each face center of the structure at equilibrium (dot shape in Figure 3).

Contrary to usual linear potential flow solver, the advantages of this approach are:

- Only relevant degrees of freedom are considered and calculated for radiation problems. n_{dof} radiation problems are solved instead of $6 \times n_{bodies}$. It saves computational time (e.g. with example of Figure 2: 12 radiation problems instead of 42).
- It is easy to consider degrees of freedom different from conventional 6 DoFs of marine structures.

Results of the hydrodynamic calculations are hydrodynamic coefficients and forces acting at joints of the multibody structures. Thus they are straightforward to use with the multibody solver. Rules for pressure surface integration leading to hydrodynamic coefficients result from the multibody solver.

Once added mass, hydrodynamic damping and diffraction force are obtained in frequency domain, time domain reconstruction is performed by a hydrodynamic postprocessor, thus generating input for the multibody solver. For now, the convolution by impulse response is used both for diffraction and damping part of the radiation force:

$$\boldsymbol{K_{diff}}(t) = \frac{1}{2\pi}\int_{-\infty}^{+\infty} \boldsymbol{F_{diff}}(\omega)e^{i\omega t}d\omega \tag{3}$$

$$\boldsymbol{f_{diff}}(t) = \int_{-\infty}^{+\infty} \boldsymbol{K_{diff}}(\tau)\eta(t-\tau)d\tau \tag{4}$$

Diffraction quantities are 6D force vectors acting on each body.

$$\boldsymbol{K_{rad}}(t) = \frac{2}{\pi}\int_{0}^{+\infty} \boldsymbol{B}(\omega)\cos(\omega t)d\omega \tag{5}$$

$$\boldsymbol{\mu}(t) = -\int_{0}^{t} \boldsymbol{K_{rad}}(\tau)\dot{\boldsymbol{Y}}(t-\tau)d\tau \tag{6}$$

Radiation quantities are treated at the scale of the multibody system. $\boldsymbol{K_{rad}}$ is a $(n_{dof} \times n_{dof})$ matrix whereas $\boldsymbol{f_{rad}}$ and $\dot{\boldsymbol{Y}}$ are vectors of size n_{dof}.

In addition, wave excitation can be modelled both by linear or nonlinear Froude-Krylov force. In case of linear Froude-Krylov force, the incident wave loads are directly added to the diffraction loads in frequency domain.

Buoyancy force can also be chosen linear or nonlinear. Morison loads model has also been implemented. Different available options are gathered in Table 1.

Force	Linear	Nonlinear
Diffraction	Yes	No
Radiation	Yes	No
Buoyancy	Yes	Yes
Froude-Krylov	Yes	Yes
Morison	Yes	

Table 1: Hydrostatic/dynamic forces available models

Wave generation

Once the hydrodynamic database has been built, simulations in waves can be performed. Different wave models are available to describe the wave kinematics:

- linear regular waves (Airy waves)
- linear irregular waves from mono/multi directional spectrum (Jonswap, Pierson-Moskovitz, …)
- Nonlinear irregular wave kinematics, calculated using the High Order Spectral program from LHEEA Lab ([9], [10]) will also be implemented.
- Finite or infinite water depth

PTO and mooring forces

Any function could be input by the user (function of velocities and positions, look-up tables…) to model the mooring forces, PTO and controls. At present time, linear elastic mooring is available. In the near future, it is actually envisaged to derive dynamic model using the same multibody dynamic formalism as the multibody solver.

VERIFICATION OF THE MODEL: CYLINDER

The aim of this section is to verify *InWave* results comparing it with a fully linear numerical model (*Aquaplus*).

Simulations were run on a single 6 DoF cylinder in small steepness (1%) regular waves, to remain in the frame of linear theory. Same mesh was used for both simulations.

Cylinder dimensions are given in Table 2.

heigth (m)	20
diameter (m)	10
mass (t)	1200
CoG (m from free surface)	-11.58
draft (m)	15.08
pitch inertia (t.m²)	1.89E+04
mooring stiffness (kN/m)	10

Table 2: Cylinder dimensions

Linear Froude-Krylov, diffraction/radiation and buoyancy are used. These quantities are all computed on the mesh at equilibrium, as depicted in Figure 4. Moreover, linear mooring along *x*-axis is added. All 6 DoFs are freed but only surge, heave and pitch are actually non-zero.

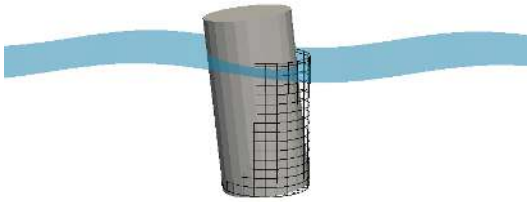

Figure 4: Instantaneous cylinder in regular waves and equilibrium mesh used for hydrodynamics loads computation

Reference

The reference results are obtained from the widely validated *Aquaplus* potential code from *Ecole Centrale de Nantes* [5]. The equation of motion of the cylinder is solved in frequency domain and the RAOs are obtained. Time series in regular waves are quickly reconstructed:

$$X(t) = -AX(\omega)\sin(\omega t + \varphi(\omega)) \qquad (7)$$

Where:

- $X(t)$ is the motion in time domain.
- A is the incident wave amplitude.
- $X(\omega)$ is the motion amplitude RAO computed in frequency domain.
- $\varphi(\omega)$ is the motion phase RAO computed in frequency domain

Impulse responses are also computed from *Aquaplus* results.

Results

Time domain simulations were run with *InWave* with linear Froude-Krylov and linear buoyancy on regular waves of 1% steepness. Water depth was set to infinite and wave periods range from 2 to 21s. Simulation time used was 1000s to ensure steady state. Time step of 0.1s was chosen. Simulation time was around 8 times real time.

Impulse responses duration was taken to 20s with a 0.05s time step. There is a good match between impulse responses computed by *Aquaplus* and *InWave*.

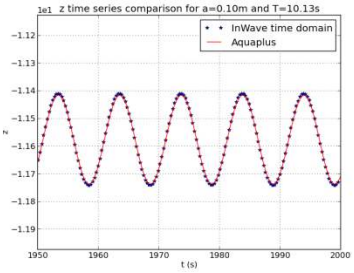

Figure 5: Comparison of cylinder heave time series in regular waves (a=0.1m, T=10.13s)

Once steady state is reached with *InWave* time domain simulations, time series of motion obtained from both software show very good agreement (see Figure 5).

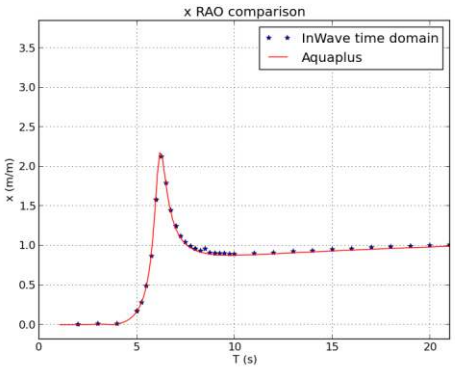

Figure 6: Comparison of cylinder surge RAOs

The RAOs are then reconstructed from time series by *InWave* post processing environment, using harmonic analysis. They also show good agreement with *Aquaplus* results (see Figure 6 and Figure 7).

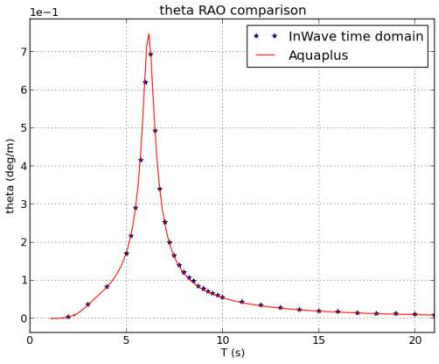

Figure 7: Comparison of cylinder pitch RAOs

To conclude, there was a very good agreement between *InWave* results and *Aquaplus* results, which gives confidence in the numerical implementation.

APPLICATION TEST CASE: F3OF SYSTEM

The aim of this part is to show the ability of *InWave* to model a complex WEC system by comparing with results obtained in *NumWec* report ([2]).

Presentation

A Langlee-like system has been chosen because it sums various difficulties:

- Base is free to move
- Strong hydrodynamic interaction between bodies
- Rotations and translations at stake

The *F3OF* system was modelled as close as possible as it was in [2]. Note that this system does not pretend to be optimal nor faithful to any commercial WEC.

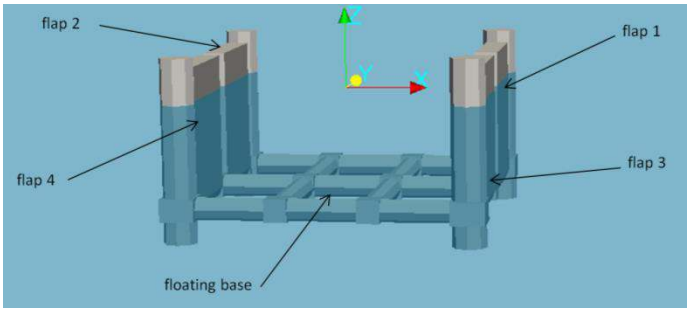

Figure 8: Visualization of F3OF system

The *F3OF* system is made of an underwater base composed of horizontal and vertical pipes. The base is anchored and is *a priori* free to move in 6 DoFs. Four flaps are fixed to this frame and can rotate around their hinges. Altogether, it forms a 10 DoFs system.

F3OF is symmetrical according to *(xOz)* plane. Flaps 1 and 3 are called rear flaps and 2 and 4 front flaps.

Main dimensions and inertial data of the F3OF are exposed in Table 3. In [2], different set of parameters have been tested. In this study, only the configuration described in Table 3 is considered for simulations in waves. It can be noticed that in this configuration, the mass of each body is not equal to its own displacement. The equality is verified on the whole system.

Base		Flaps	
length (m)	25	thickness (m)	2
width (m)	25	width (m)	9.5
draft (m)	12	draft (m)	10
displacement (m3)	673	displacement (m3)	184.4
mass (t)	1090	mass (t)	89.6
CoG (m from free surface)	-9	hinge (m from free surface)	-9
		CoG (m from hinge)	4.75
pitch inertia (t.m²)	7.63E+04	pitch inertia (t.m²)	650
mooring stiffness (kN/m)	100	PTO damping (kN.m.s)	2.00E+04

Table 3: F3OF main dimensions

Numerical modeling

The frame of reference is placed above the geometric center of the system, such that the free surface at rest is the zero of *z*-axis (see Figure 8).

In this study, mono-directional waves propagating along *x*-axis are considered. Therefore, only surge, heave and pitch DoFs are activated for the base body. Water depth is assumed to be infinite.

The following forces are applied to the system:

- gravity;
- nonlinear buoyancy;
- linear excitation and diffraction force;
- linear radiation force;
- linear mooring along *x*-axis on the base body;
- linear power take-off on each flap hinge;
- Morison drag is added on each body as it is done in [2].

The mesh used for hydrodynamic computations contains 1930 vertices and 1792 faces. It is displayed in Figure 9. Mesh convergence has been checked with a finer mesh (2584 faces) by comparing *Nemoh* results on both meshes.

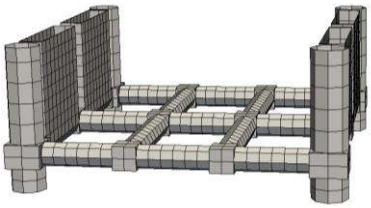

Figure 9: Hydrodynamic mesh of the F3OF used for *InWave* simulations

The mesh used is the same as the one used in [2]. Generally speaking, it was intended to reproduce what was done in [2]. Anyway, some main differences remain between the two models. They are exposed in Table 4.

NumWec	***InWave***
System-specific motion equations are written	General multibody equations are used
$6 \times n_{bodies}$ radiation problems are solved by BEM	n_{dof} radiation problems are solved by BEM
Equation of motion is linearized	Motion equation is fully non-linear
Linear buoyancy is used	Non-linear buoyancy is used

Table 4: Model differences between *NumWec* and *InWave*

Frequency domain results

Raw frequency domain results obtained with *InWave* have been compared with the ones presented in [2]. They show very good agreement, as shows an example in Figure 10.

Impulse responses are also very similar. Figure 11 shows the example of heave radiation impulse response when the whole structure moves along *z*-axis.

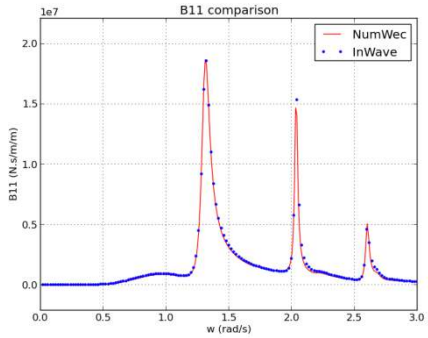

Figure 10: Comparison of hydrodynamic damping in surge created when the whole structure moves in surge

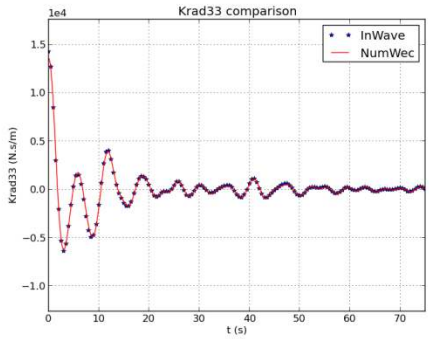

Figure 11: Comparison of heave impulse response when the whole structure moves in heave

As shows Figure 12, impulse responses of one flap to the one in front are very long to decay. On the other hand, the impulse responses duration is very critical for the overall simulation time. A trade-off had to be made and the duration of impulse responses was taken to 200s, with a time step of 0.05s.

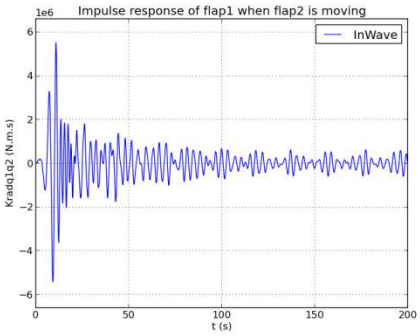

Figure 12: Flap 1 impulse response to flap 2 motion

Decay tests

To get confidence in the numerical model, simple decay tests have been performed. Such simulations are performed in still water (thus no excitation/diffraction force is used). The system is shifted from its equilibrium position along a single DoF and released. It is expected to describe damped oscillations back to equilibrium position. The oscillations should be at the natural frequency of the corresponding DoF:

$$\omega_0 = \sqrt{\frac{K_h + K_m}{M + M_a}} \tag{8}$$

With:

- K_m: the mooring stiffness (if any)
- K_h: the hydrostatic stiffness
- M: the mass (or inertia in rotation)
- M_a: the added mass

The first experiment performed is a flap decay test with a fixed base. All PTOs are switched off. The mass of the flap and base is modified for this experiment, to fit the configuration used in [2]. Mass of the flaps is set to 139.6t and the one of the base to 889.8t. Both rear flaps are opened by pushing them with a constant force F_x until they reach a stable position. At t=0, F_x is removed which releases the flaps. Figure 13 and Figure 14 show the position time series of flaps 1 and 2.

Several things can be noticed:

- Damped oscillations are indeed observed for flap1.
- The period of these oscillations is measured to 20.0s, which corresponds to the natural period (19.8s) computed with (8) and the one found in [2] (19.5s).
- Flap 2 is excited by flap 1 and responds at the same period.
- Flap 2 oscillations are increasing at first then decreasing.

A heave decay test was also performed on the whole system. The flaps are artificially fixed by setting an "infinite" value for all PTOs. A constant force F_z is applied and released at t=0. The heave decay period is measured to 9.2s, which again corresponds to the natural period (9.1s) obtained from equation (8) and with [2] (9.4s).

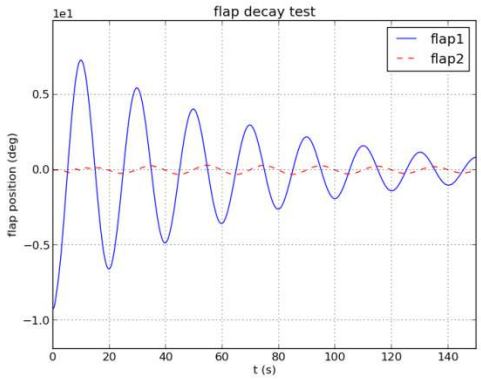

Figure 13: Time series of flaps 1 and 2 during flap 1 decay test

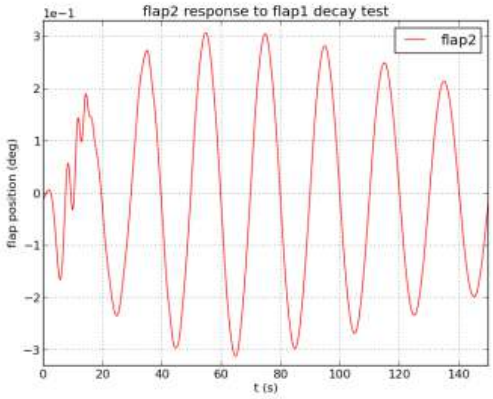

Figure 14: Flap 2 response to flap 1 decay test

Regular wave results

Dynamic simulations have been conducted in 21 linear regular waves of constant amplitude (a=1m) with periods ranging in 5-15s. Simulation time was taken to 1000s with a time step of 0.1s. The first 400s are discarded to keep only steady state. Each wave simulation could be run in parallel processors.

Motion RAOs are constructed by harmonic analysis of the motion time series. Power RAOs are obtained taking the time average of the instantaneous extracted power.

Results are compared with the RAOs exposed in [2] with the same system configuration. Table 4 recalls the main differences between the 2 numerical models.

Figure 15 shows the RAO of base body pitch motion. It shows quite good agreement between *InWave* and *NumWec* results.

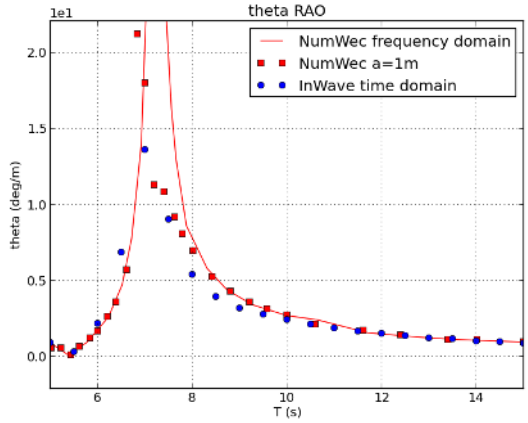

Figure 15: F3OF pitch RAOs comparison

Figure 16 shows the comparison of RAOs for flap 1. They also show fair agreement.

Finally, Figure 17 shows the total extracted power RAO obtained from *InWave* and *NumWec* simulations with the same PTO configuration. Here again, there is a good match between the different models.

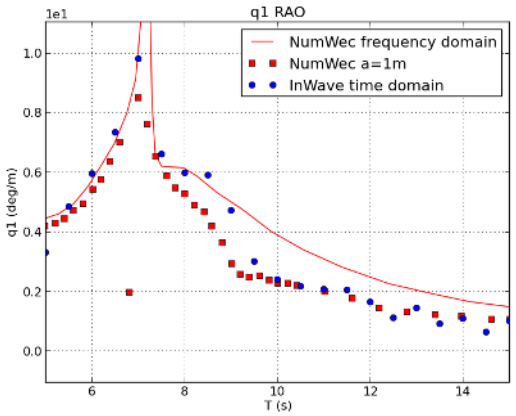

Figure 16: F3OF flap 1 RAOs comparison

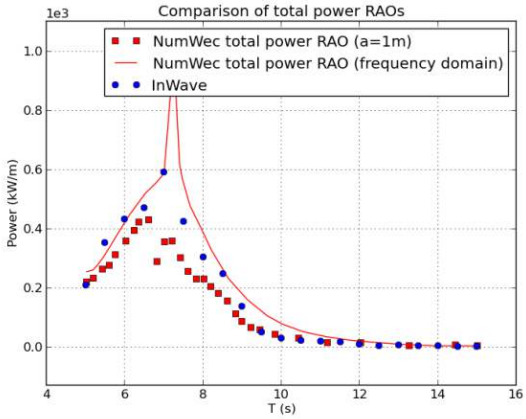

Figure 17: F3OF extracted power RAOs comparison

In [2] RAOs have been computed in frequency domain and time domain. Frequency domain results RAOs are unphysical at resonance as no viscosity is modeled. Adding Morison viscous drag in time domain simulations is damping resonances.

Despite the difference of approaches between both numerical models, these comparisons show fair agreement. It verifies the coupling between the time domain multibody solver and the frequency domain hydrodynamic solver. It also increases the confidence in algorithms used in *InWave* as well as their implementation.

Irregular wave results

Irregular waves are generated from Jonswap for different values of significant wave height (Hs) and peak period (Tp). The "peakness" parameter (γ) is always taken to 3.3. Irregular waves are obtained from 300 regular wave frequencies from 0.2 to 3 rad/s. With such configuration, the wave signal is expected to repeat itself after 600s.

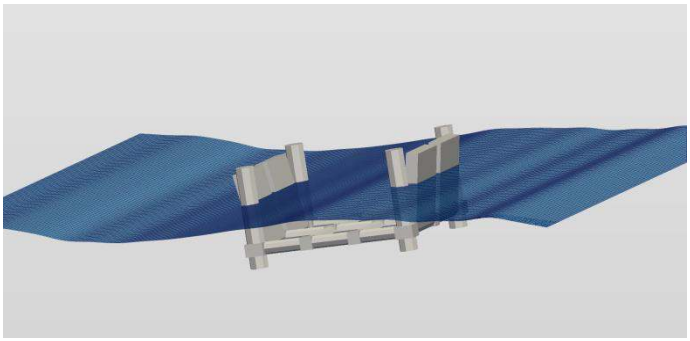

Figure 18: Visualization of the F3OF device in irregular waves

Simulations were run on 1000s with a time step of 0.1s. First 400s are discarded to keep 600s without transient effect. The extracted power on one given sea state is computed as the average of the instantaneous extracted power on this time window.

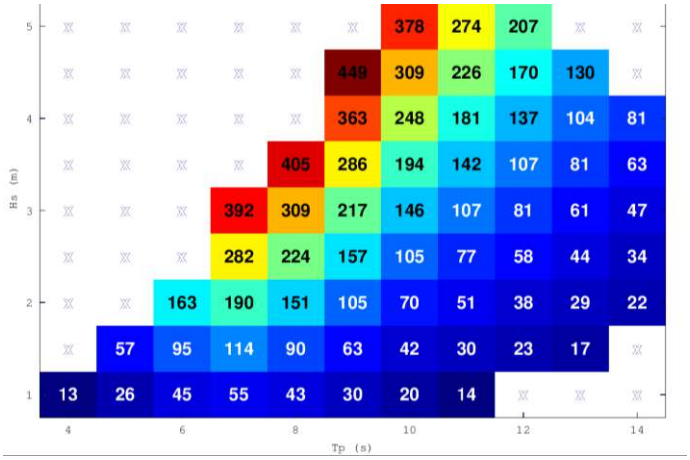

Figure 19: Power matrix obtained with *InWave*

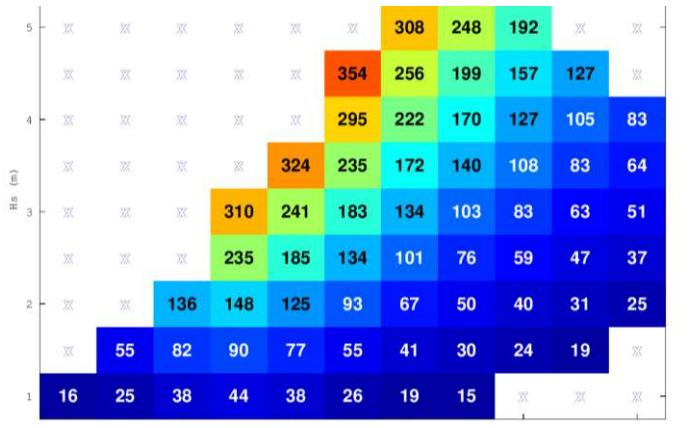

Figure 20: Power matrix obtained from *NumWec* model

A matrix is built gathering the values of extracted power, for a set of sea states *(Hs, Tp)* likely to happen at *Yeu* site (France). The same matrix was built from *NumWec* model with the same wave spectrums and PTO configuration. Both matrices are displayed in Figure 19 and Figure 20.

Extracted power values in irregular obtained with *InWave* and *NumWec* also show quite good agreement. Trends are similar and maximums are located in the same place in the diagrams.

Differences were expected to grow with wave steepness, as *InWave* model introduces some nonlinearity (in buoyancy term and equation of motion) that is not present in *NumWec* model. Indeed, it can be observed in Figure 19 and Figure 20 that the bottom-right triangles of the power matrices (small steepness waves) match better than the top-left triangles. In fact, the top-left cells correspond to large structure motion due to both large amplitude and wave periods close to resonance. With growing flap angles, the underwater profile of the structure is significantly changing. Taking into account nonlinear buoyancy is thus expected to impact the results when large motions are happening.

These results again give confidence in *InWave* model.

CONCLUSION

In this article, *InWave* theory was exposed. It was shown how it addresses the problem of complex WEC systems modelling, thanks to a complete multibody approach.

Results were verified on a basic test case comparing *InWave* with the widely validated seakeeping code *Aquaplus*.

A full test case has finally been presented on a complex Langlee-like WEC. Successful comparison was performed with results obtained from [2].

This study shows that the novel algorithms implemented in *InWave* are relevant and increase the confidence in the code.

After this first model to model validation, *InWave* will be largely tested. Validation against experimental results is currently undergoing and will soon be published.

REFERENCES

[1] F. Rongère, A. Clément. “Systematic Dynamic Modeling and Simulation of Multibody Offshore Structures: Application to Wave Energy Converters”, OMAE2013-11370, Nantes, France.

[2] A. Babarit, J. Hals, M.J. Muliawan, A. Kurniawan, T. Moan, J. Krokstad. “Numerical benchmarking study of a selection of wave energy converters”, Final technical report, 2011.

[3] F. Rongère, A. Babarit, A. Combourieu, A.H. Clément, “Time Domain Simulation of Multibody Floating Offshore Structures with Hydrodynamic Interactions”, to be submitted for publication.

[4] E. Mackay, J. Cruz, M. Livingstone, P. Arnold. “Validation of a Time-Domain Modelling Tool for Wave Energy Converter Arrays” in EWTEC 2013 Proceedings of 10th European Wave and Tidal Energy Conference, Aalborg, Denmark, 2-5 September, 2013, p.12.

[5] G. Delhommeau. “Seakeeping codes Aquadyn and Aquaplus”. In Proc. Of the 19th WEGEMT school, numerical simulation of hydrodynamics: ships and offshore structures, 1993.

[6] W. Khalil and J. Kleinfinger. “A new geometric notation for open and closed-loop robots”. In 1986 IEEE International Conference on Robotics and Automation. Proceedings, volume 3, 1986.

[7] A. LaBonte et al. “Wave Energy Convertor Simulation: Development, Code Competition, and Validation Efforts” in EWTEC 2013 Proceedings of 10th European Wave and Tidal Energy Conference, Aalborg, Denmark, 2-5 September, 2013, p.16.

[8] K. Shoele, M. Previsic. “A Novel Simulation Toolbox for Wave Energy Converters” in EWTEC 2013 Proceedings of 10th European Wave and Tidal Energy Conference, Aalborg, Denmark, 2-5 September, 2013, p.15

[9] Ducrozet, G., Bonnefoy, F., Touz´e, D. L., and Ferrant, P., 2012. “A modified high-order spectral method for wavemakermodeling in a numericalwave tank”. European Journal of Mechanics - B/Fluids, 34(0), pp. 19 – 34.

[10] Ducrozet, G., Bonnefoy, F., Le Touz´e, D., and Ferrant, P., 2007. “3-d hos simulations of extreme waves in open seas”. Natural Hazards and Earth System Science, 7(1), pp. 109–122.

[11] J. Newman, 1994, “Wave effects on deformable bodies”, Applied ocean research 16(1), 47-59

[12] http://lheea.ec-nantes.fr/doku.php/emo/nemoh/start